



This item was submitted to Loughborough's Institutional Repository (<https://dspace.lboro.ac.uk/>) by the author and is made available under the following Creative Commons Licence conditions.


C O M M O N S D E E D

Attribution-NonCommercial-NoDerivs 2.5

You are free:

- to copy, distribute, display, and perform the work

Under the following conditions:



Attribution. You must attribute the work in the manner specified by the author or licensor.



Noncommercial. You may not use this work for commercial purposes.



No Derivative Works. You may not alter, transform, or build upon this work.

- For any reuse or distribution, you must make clear to others the license terms of this work.
- Any of these conditions can be waived if you get permission from the copyright holder.

Your fair use and other rights are in no way affected by the above.

This is a human-readable summary of the [Legal Code \(the full license\)](#).

[Disclaimer](#) 

For the full text of this licence, please go to:
<https://creativecommons.org/licenses/by-nc-nd/2.5/>

1 **Maximizing the accuracy of image-based surface sediment**
2 **sampling techniques**

3 David J. Graham¹, Anne-Julia Rollet², Hervé Piégay³, Stephen P. Rice¹

4

5 ¹Department of Geography, Loughborough University, Loughborough, LE11 3TU UK.

6 ²Aix-Marseille université, CEREGE – CNRS UMR 6635 France.

7 ³University of Lyon, CNRS, UMR 5600, Site ENS-lsh, Lyon, France

8

9 Corresponding author: David Graham (D.J.Graham@lboro.ac.uk)

1 Recent years have seen increased interest in automated methods, utilizing photographs
2 collected with a hand-held digital camera, for determining the grain-size distribution of coarse
3 river sediments. Such methods are as precise as traditional field methods, and have
4 considerable time and cost advantages. Nevertheless, several unresolved issues pertaining to
5 their deployment remain to be addressed. Using datasets collected from seven gravel-bed
6 rivers, this paper examines four key issues: (i) the minimum area required to obtain a
7 representative sample; (ii) the effect of lower-end truncation on grain-size percentiles; (iii) the
8 effect of river-bed structure such as imbrication and hiding; and (iv) the potential benefits of
9 using individual particle measurements rather than the number (or mass) of particles per size
10 class to calculate percentiles. It is demonstrated that sampling areas of between 50 and 200-
11 times that of the largest grain are adequate to achieve percentile errors of <10% (in mm). The
12 appropriateness of lower-end truncation depends on the study aims and sediment properties. It
13 has a limited effect on higher percentiles, except where sand is a major constituent.
14 Understanding the influence of bed structure on image-derived size information is
15 complicated by the absence of error-free benchmarks against which accuracy may be
16 evaluated, but it is likely that other errors are more important. The use of individual particle
17 measurements to calculate percentiles in preference to classified data is shown to have a
18 small, but appreciable, effect on precision. These results will assist practitioners in making
19 appropriate operational decisions to maximize data quality using image-based grain-size data
20 capture.

21

1 **1. Introduction**

2 The grain-size distributions of coarse sediments exposed on river beds, and elsewhere, are
3 important in a variety of geomorphic, ecological and engineering contexts. Characterization of
4 coarse-grained size distributions using traditional field methods like pebble counts, paint-and-
5 pick and adhesive sampling [*Wolman, 1954; Lane and Carlson, 1953; Diplas and Fripp,*
6 1992] is time-consuming and costly, and destroys the surface being sampled. It is therefore
7 often impracticable, using these techniques, to resolve important spatial variability and
8 temporal changes in surface grain size. However, recent advances in image-analysis have seen
9 the rapid development and adoption of alternative techniques that use the analysis of surface
10 images to overcome the limitations of traditional methods [*Graham et al., 2005b; Marcus and*
11 *Fonstad, 2008*]. These methods, which build on earlier photographic sampling procedures
12 [e.g. *Adams, 1979; Ibbeken and Schleyer, 1986*], are non-invasive and can provide grain-size
13 information at a quality comparable to that from traditional techniques. Their key advantage is
14 the rapidity with which data may be collected and analyzed. This rapidity facilitates data
15 collection at higher spatial and temporal resolutions, and across larger areas than are possible
16 using traditional methods, all of which are hugely beneficial in understanding geomorphic
17 processes.

18 There are two major approaches to image-based granulometry at present. The first provides
19 ensemble grain-size parameters (e.g. the D_{50} for an area) based on evaluating the spectral
20 characteristics or semivariance structure of imagery, principally from airborne platforms
21 [*Carbonneau et al., 2004; Chandler et al., 2004; Verdu et al., 2005*]. This is proving to be a
22 valuable method for mapping grain-size variations at a reach scale. [*Carbonneau, 2005;*
23 *Hedger et al., 2006*]. *Rubin [2004]* and *Buscombe and Masselink [2009]* have developed
24 similar systems for examining sand-bed grain-size parameters at scales of a few centimeters.

1 This technology has been extended for application on gravel-sized particles [*Adams et al.*,
2 2007; *Ruggiero et al.*, 2007].

3 The second approach applies semi- and fully-automated object-detection algorithms to images
4 collected by ground-based photography to obtain grain-size measurements of the individual
5 grains in an image and thereby produce a complete grain-size distribution. *Butler et al.*
6 [2001], *Reid et al.* [2001] and *Sime and Ferguson* [2003] demonstrated that this approach
7 could provide detailed grain-size information at bar and reach scales. Subsequently, *Rollet*
8 [2007] applied a semi-automated procedure to assess the impact of a sediment deficit
9 associated with dam construction on downstream grain-size characteristics along a 40 km
10 river reach (incorporating 109 bars). *Graham et al.* [2005a, 2005b] developed a fully-
11 automated and transferable algorithm which optimizes results for a variety of sediment types.

12 This paper focuses on these discrete-grain techniques and uses field data to examine several
13 important issues related to their deployment that have not, to date, been fully assessed. These
14 issues relate to procedures for minimizing errors associated with each of the three stages of
15 photographic data capture: collection of images; extraction of grain sizes; and analysis of the
16 results (Fig. 1). Whilst some work has examined these issues in the context of the manual
17 digitization of photographs [e.g. *Kellerhals and Bray*, 1971; *Ibbeken and Schleyer*, 1986;
18 *Bunte and Abt*, 2001a], several issues are unresolved in the context of automated methods.
19 Although these issues are discussed here in the context of developing better use of automated
20 image-based methods, several of them are also of relevance for the accurate estimation of
21 grain-size distributions using traditional methods. In particular this paper examines the effect
22 of several procedures on the grain-size distributions: the choice of sampling area; the effect of
23 applying a truncation to small grains; and the use of discrete particle measurements versus
24 measurements that bin particles into size classes. We also examine how hiding and

1 imbrication of surface particles affect grain-size distributions. These are important
2 considerations because of the anticipated growth in the adoption of image-based techniques
3 by scientists and practitioners. We utilize data collected on seven gravel-bed rivers of
4 contrasting bed-material lithology and character: Ettrick Water (Scotland), Afon Ystwyth
5 (Wales), River Lune (England), the Ain River (France), and the Fraser, Chilliwack and Peace
6 Rivers (Canada).

7 **2. Sampling area and sample size**

8 **2.1 Rationale**

9 All grain-size measurement approaches are limited, to a greater or lesser extent, in the range
10 of grain sizes that can be measured. Such limitations may result in truncation of the upper or
11 lower part of the grain-size distribution, or introduce a size-dependent bias in the measured
12 distribution as a result of inadequate characterization of fine or coarse grains. The size of
13 particles that can be measured by image-based techniques is limited by the area covered in the
14 image (at the coarse end) and the resolution of the image (at the fine end). Truncation of the
15 coarse end of the distribution may be avoided by photographing a larger area (either by
16 increasing the area of individual images, or montaging multiple images). Issues surrounding
17 truncation at the fine end of the distribution are discussed in the next section.

18 In order to avoid inadvertent truncation of the coarse end of the grain-size distribution, all
19 sampling methods must include sufficient grains to adequately represent the population being
20 studied. One approach to achieving this is to photograph the entire area of interest using
21 multiple images. This would allow the continuous variation in grain size across the surface to
22 be established, and permit investigation of the ways in which surface texture varies at scales

1 from the individual grain to an entire bar. The ability to undertake such analyses is a
2 significant benefit of image-based sampling over traditional methods. More often, however, a
3 more focused sampling strategy will be employed to characterize the properties of a particular
4 facies or assess spatial trends in grain-size attributes. In such cases it is desirable to use the
5 smallest sample sizes that are adequate to represent the populations of interest. This is to
6 minimize sampling effort and to reduce the probability of inadvertently sampling across areas
7 within which there is a textural gradient.

8 There is a considerable body of literature on the sample sizes required for representative grid
9 surface sampling [e.g. *Fripp and Diplas*, 1993; *Rice and Church*, 1996; *Petrie and Diplas*,
10 2000] and volumetric sampling of the subsurface [*De Vries*, 1970; *Church et al.*, 1987; *Fripp*
11 *and Diplas*, 1993; *Rice and Haschenburger*, 2004; *Haschenburger et al.*, 2007]. Much less
12 attention has been paid to criteria for representative areal sampling.

13 The number of grains required in an areal sample is considerably larger than in a grid sample
14 of similar precision [*Petrie and Diplas*, 2000]. However, because areal samples are based on
15 predefined areas (cf. grid samples, which consist of a predefined number of grains), guidance
16 on appropriate sample sizes is most usefully given in terms of the area to be sampled rather
17 than the number of grains to be included. This sampling area has commonly been defined as a
18 function of the area of the largest particle of interest. *Diplas and Fripp* [1992] proposed that a
19 sampling area at least 100 times the area of the largest particle should be used to obtain a
20 precision equivalent to a 100-grain grid sample. *Fripp and Diplas* [1993] argued that a
21 sampling area 400 times the that of the largest particle is required to meet the ‘low precision’
22 criterion of *De Vries* [1970], giving a relative error of 10%. A more sophisticated approach
23 was introduced by *Petrie and Diplas* [2000], based on the multinomial distribution and the
24 application of a two-stage sampling procedure. This is rather complex to apply in practice,

1 and requires the collection of an initial grid sample, which negates many of the benefits of
2 photographic areal sampling. Nevertheless, the results of their analysis indicated that even the
3 100-times criterion of *Diplas and Fripp* [1992] is overly conservative, and substantially
4 smaller sampling areas are acceptable.

5 The relative ease with which photographic samples can be collected facilitates the collection
6 of many samples in a short time. Where rapid fully-automated measurement procedures are
7 used, taking only a minute or two per image, it is feasible to combine size information from
8 multiple images to achieve acceptable truncation at the fine end whilst sampling an area large
9 enough to be representative of the population. This may be appropriate in many cases, but
10 where characterizing small-scale spatial variability in grain-size is the objective of the study it
11 is essential that the area sampled has experienced similar local hydraulic conditions, and must
12 therefore be as small as possible (whilst still being large enough to representatively sample
13 the full grain-size distribution) [*Rollet et al.*, 2002; *Rollet*, 2007]. Furthermore, where manual
14 or semi-automatic measurement of the images is used, increasing the number of images adds
15 substantially to the processing time and may negate many of the benefits of photographic data
16 collection (although expensive field time will still be reduced). Other types of areal sampling
17 procedure (e.g. paint-and-pick; clay; wax) may sometimes be desirable, but these are
18 particularly time and labor intensive in both the field and laboratory.

19 For their fully-automated image-based analysis method, *Graham et al.* [2005a] determined
20 that the smallest grain of interest (i.e. the lower-end truncation) should have a diameter larger
21 than 23 pixels in the image, although this limit can probably be relaxed slightly for processes
22 where there is operator intervention. If the criterion is applied in a study with a truncation at 8
23 mm and using an 8 MP camera, the largest area that could be included in a single image is
24 0.97 m^2 . Assuming that the area of a grain is equal to the square of its *b*-axis and applying the

1 100-times criterion of *Diplas and Fripp* [1992], the D_{\max} particle size must be smaller than 99
2 mm if a representative sample is to be obtained. If the 400-times criterion of *Fripp and Diplas*
3 [1993] is applied, the D_{\max} size must be less than 49 mm. Seven photographs are required
4 when sampling a surface containing large cobbles (up to 256 mm) to meet the 400-times
5 criterion.

6 These issues mean that the development of clear guidelines on the sampling area required to
7 meet the precision requirements of a particular study is highly desirable, preferably in a form
8 readily applied in the field.

9 **2.2 Empirical assessment of minimum area for representative sampling**

10 The ease of photographic sampling facilitates the empirical evaluation of the various size
11 criteria for areal samples. The effect of sample area on the precision of key percentiles was
12 assessed using eight patches, each with an area of 12.75 m², on two bars at the Afon Ystwyth,
13 Wales. Each patch (representing the population grain size against which samples with
14 different areas are compared) was selected to have no visually discernable systematic
15 variation in grain-size distribution across it. Subsequent analysis revealed that four of the
16 patches did have statistically significant variations in either the D_{50} or D_{90} across them, but in
17 all cases the magnitude of these variations was extremely small. The D_{50} of the patches
18 ranged from 4.4 Psi (21 mm) to 5.1 Psi (35 mm) and they were moderately sorted (inclusive
19 graphic standard deviation between 0.7 and 1.0 Psi). Every patch was divided into 50 sample
20 areas, each with an area of 0.255 m². The sample areas were photographed vertically with a
21 hand-held digital camera and the images analyzed using the procedure of *Graham et al.*
22 [2005a, 2005b], the grain-size distributions being truncated at 8 mm.

1 For each patch, a random sample was chosen and the difference in its D_{50} and D_{90} relative to
2 the whole patch (population) was calculated. This was repeated for increasingly larger sample
3 areas, aggregating percentiles for two randomly selected samples, then three, then four etc.
4 Each repeat produces an estimate of the error in percentile values (relative to the population)
5 associated with a particular sample area. Because the results of this procedure vary slightly
6 each time it is undertaken, it was repeated 10 times for each patch to overcome random
7 effects. Areal samples are often collected for the purpose of comparison with data derived
8 from grid sampling, so percentile errors were calculated in both area-by-number and grid-by-
9 number form (the method for calculating grid-by-number percentiles where the area and b -
10 axis of each grain are known is described by *Graham et al.* [2005b]). For each permutation,
11 the ratio between the sampled area and the area of the largest grain in the population was also
12 calculated. Figures 2 (area-by-number percentiles) and 3 (grid-by-number percentiles) present
13 covariant plots of the magnitude of the percentile errors (expressed as percentages in mm)
14 against these ratios and provide an indication of the sample area (relative to the area of the
15 largest grain) required for the errors to stabilize to low values.

16 **Figure 2.**

17 **Figure 3.**

18 As expected, the results indicate a strong relation between sampled area and the precision of
19 the D_{50} and D_{90} (summarized in Table 1). Where data are required in area-by-number form
20 (Fig. 2) they suggest that the sample area should be at least 100-times greater than that of the
21 largest particle to achieve D_{50} errors of less than 5% in mm (0.07 Psi). To achieve equivalent
22 precision in the D_{90} , the sample area should be greater than 200-times that of the largest
23 particle. To achieve errors of less than 10% in mm (0.14 Psi) sample areas of around 100-

1 times that of the largest grain are acceptable. Larger sampling areas are required to achieve
2 similar errors in grid-by-number percentiles because of the greater weight placed on larger
3 grains in such distributions (Fig.3).

4 Caution should be exercised before extrapolating these results to other locations with different
5 textural and sorting characteristics. Nevertheless, the results do suggest that the small sample
6 areas proposed by *Petrie and Diplas* [2000] may be insufficient. For higher precision, larger
7 percentiles and grid-by-number data, areas as large as 400-times that of the largest grain
8 (which for practical purposes may be approximated by the square of the *b*-axis length) may be
9 required. Practitioners will need to balance the competing demands of precision and field time
10 within the context of their project requirements.

11 **3. The importance of truncation**

12 **3.1 Rationale**

13 In practice, it is relatively easy to avoid problems associated with inadequate characterization
14 of the coarse fraction because the presence of large grains is easily recognized and steps can
15 be taken to adjust the sampling strategy to include them. Bias or truncation at the fine end of
16 the distribution is likely to be a more significant problem because its effects may not be so
17 easily recognized. In the context of image-based techniques, the minimum resolvable grain
18 size is controlled by the resolution of the image. Although continual increases in digital
19 camera resolution will result in improvements in the ability to recognize small grains, there
20 will always be a lower limit to the size of grains that can be identified reliably and measured
21 accurately using image-based methods. For the fully-automated technique of *Graham et al.*
22 [2005b], measurement error increased substantially for grains with an apparent *b*-axis smaller

1 than 23 pixels in the image. Such issues are not limited to new sampling techniques. It is well
2 established, for example, that grid-by-number samples [*Wolman, 1954*] commonly result in
3 under representation of fine grains as a result of operator bias [*Diplas and Fripp, 1992; Fripp*
4 *and Diplas, 1993; Marcus et al., 1995*]. As a result, it is common practice to truncate grid-by-
5 number samples at a size above which the operator is confident that bias is no longer present
6 (often 8 mm [*Rice, 1995*]).

7 Although size-dependent bias may be acceptable in some circumstances (e.g. where having
8 biased data is considered better than no data), in most cases a truncation is required to ensure
9 that only representatively sampled grains are included in the derived size distribution [*Church*
10 *et al., 1987*]. Where samples are being compared, it is essential that a common range of
11 representatively sampled grains is used, which will usually require a truncation to be applied
12 to one or both data sets. However, the application of truncations can be problematic because
13 truncation modifies, to a greater or lesser extent, the entire cumulative grain-size distribution
14 curve used to determine percentiles [*Bunte and Abt, 2001b*]. Indeed, *Fripp and Diplas* [1993,
15 p. 478] argued that “the hazards of using truncated samples cannot be overstated”. Some
16 applications, such as calculation of the bedload transport fluxes [*Reid et al., 1996*], are highly
17 sensitive to small variations in percentiles. What then is the magnitude of the error introduced
18 by truncation (either intentional or inadvertent) of the distribution?

19 **3.2 Empirical assessment of the impact of truncation**

20 The effect of lower-end truncation was tested using a dataset consisting of 74 grid-by-number
21 samples, each of around 300 grains, collected from three Canadian rivers (Fraser, Chilliwack,
22 Peace). Grids with intervals greater than twice the largest grain diameter were laid out with
23 tapes and particles to be sampled were identified as those lying below relevant tape

1 graduations. For each sample, the number of grains smaller than 1 Psi (2 mm) was recorded
2 and larger particles were assigned to half Psi classes using templates. The D_{50} of the samples
3 ranges from 4.2 Psi (18.4 mm) to 7.1 Psi (137 mm) and sorting from moderately well sorted
4 to very poorly sorted (inclusive graphic standard deviation ranges from 0.6 Psi to 2.1 Psi).
5 Grain-size percentiles were calculated for the raw data (Fig. 4), and for the data truncated at 1
6 Psi (2 mm), 3 Psi (8 mm) and 5 Psi (32 mm). Percentiles were calculated in Psi units and
7 spline interpolation was used to smoothly interpolate between class boundaries. The
8 differences between the percentiles from the raw and truncated data were then calculated,
9 giving the error at each percentile for each sample (upper panels in Fig. 5). The mean errors at
10 every 5th percentile (lower panels in Fig. 5) provide a clear indication of the magnitude of the
11 likely errors associated with any particular truncation and percentile. Several of the samples
12 had significant proportions of sand within them (commonly inducing a substantial
13 bimodality), resulting in substantial errors in lower percentiles when truncated. To examine
14 this effect, those samples with $> 5\%$ sand ($n = 8$) were separated from the remainder of the
15 samples (indicated by dashed lines in Fig. 5), and the mean errors in the percentiles examined
16 separately for each group.

17 **Figure 4.**

18 **Figure 5.**

19 For samples without significant quantities of sand, for an 8 mm (3 Psi) truncation, the mean
20 error in the D_{50} is -0.06 Psi (-4.2% in mm), and for a 32 mm (5 Psi) truncation the error is -0.2
21 Psi (-14.9% in mm). For those with $>5\%$ sand, the mean error in the D_{50} with a 32 mm (5 Psi)
22 truncation is -0.3 Psi (-23.1% in mm). As would be expected, the errors for lower percentiles
23 are substantial for sandy samples (Fig. 5). Whether this is acceptable depends on the

1 application, but for many purposes (e.g. as a proxy for roughness or to determine median
2 grain size) truncated data are likely to provide acceptable estimates of the true grain-size
3 percentiles. Indeed, where minor quantities of sand have been draped over the surface during
4 waning flows, it may be advantageous to ignore this component of the grain-size distribution
5 for some applications.

6 **4. The effect and significance of river-bed structure**

7 **4.1 Rationale**

8 In most surface sampling techniques, grains are removed from the substrate and their true
9 dimensions are therefore revealed prior to measurement. In contrast, photographic techniques
10 operate on grains in situ, and only the exposed parts of the grain can be measured. Given that
11 it is those parts of grains that are visible in photographs that actually interact with the flow,
12 this may not be considered a significant problem for some applications. Nevertheless, this
13 property of photographic methods has the potential to underestimate the true size of
14 individual grains as a result of three factors related to the structure of the river bed: (i) partial
15 burying of grains (the ‘iceberg’ effect); (ii) overlapping of grains as a result of imbrication;
16 and (iii) foreshortening, where the size of a grain appears smaller than it really is when
17 viewed from an angle (Fig. 6). These potential sources of bias have been recognized since
18 photographic sampling was first used [e.g. *Kellerhals and Bray*, 1971; *Ibbeken and Schleyer*,
19 1986; *McEwan et al.*, 2000], but the reported magnitude of the resulting errors have varied
20 substantially (Table 2). Furthermore, assessing of the effects of sediment structure is
21 challenging because of errors associated with the methods used to collect the control data.

22 **Figure 6.**

1 **Table 2.**

2 **4.2 Empirical assessment of the impact of river-bed structure**

3 We quantified the magnitude of these structural effects at the Ain River, France, using 10
4 patches, each of 0.6 m², at which we observed moderate imbrication. Each patch was
5 photographed vertically with a digital camera, spray painted, and all painted grains larger than
6 8 mm were returned to the laboratory and graded using square-hole sieves, the number of
7 grains in each size class being recorded. The photographs were digitized manually on screen
8 by a single operator using Adobe® Illustrator® (Fig. 7) and the apparent grains then
9 measured automatically using Scion Image. The photographs were also analyzed using the
10 semi-automatic process of *Rollet et al.* [2002]: (i) grayscale images were converted into
11 binary form by the application of a threshold, the value of which was set at a level that the
12 operator judged to be optimal; (ii) the binary image was skeletonized by the application of a
13 watershed segmentation algorithm [*Digabel and Lantuéjoul, 1977; Soille, 2002*]; and (iii) the
14 resulting objects were labeled and measured. Because the size measured by square-hole sieves
15 is influenced by grain flatness (the ratio of the *c*-axis to the *b*-axis), a correction must be
16 applied to image-based measurements to permit direct comparisons with the data derived by
17 sieving [*Church et al., 1987*]. The appropriate correction is shape dependent, but *Graham et*
18 *al.* [2005b] demonstrated that the correction factor is rather insensitive to the range of shapes
19 commonly associated with fluvial sediments and that a factor of 0.8 (equivalent to a *c*-axis to
20 *b*-axis ratio of 0.71) is generally appropriate for conversion from image-based to sieve-based
21 measurements. After the application of the sieve correction, both the digitized and sieved data
22 were truncated at 8 mm. It was judged that this was the effective limit of both reliable
23 digitization of the image and collection of painted grains in the field. The errors associated
24 with the image-based measurements were assessed with reference to seven commonly-used

1 percentiles ($\Psi_{10, 16, 25, 50, 75, 84, 90}$). Errors are defined following *Sime and Ferguson* [2003].
2 Mean error, or procedure bias, b , is defined as $b = \frac{1}{n} \sum (\Psi_{xi} - \Psi_{xp})$ where n is the sample size
3 (number of patches multiplied by number of percentiles used), Ψ_{xi} is a percentile derived
4 from the image, and Ψ_{xp} is the equivalent percentile derived from the paint-and-pick data. The
5 mean square error, E_{ms} , is defined as $E_{ms} = \frac{1}{n} \sum (\Psi_{xi} - \Psi_{xp})^2$ and the irreducible random error,
6 e , an indication of scatter, as $e = \sqrt{E_{ms} - b^2}$.

7 **Figure 7.**

8 Consistent with earlier work [e.g. *Butler et al.*, 2001; *Graham et al.*, 2005b], the number of
9 grains identified in the images is substantially fewer in all size classes than obtained by paint-
10 and-pick sampling (Fig. 8). These studies found that, despite undercounting, the precision of
11 the grain-size percentiles was excellent because the depletion was approximately uniformly
12 distributed.

13 **Figure 8.**

14 Contrary to the expectation that the sediment structure will lead to an underestimation of grain
15 sizes by image-based approaches, percentiles of the manually-digitized grains tend to
16 overestimate those from paint-and-pick sampling when presented in their original area-by-
17 number form. Typical grain-size distributions obtained by paint-and-pick sampling and
18 manual digitizing are illustrated in Figure 9 for a single sample. The relation between the
19 percentiles derived by the two methods for all samples is illustrated in Figure 10a. The mean
20 error in the seven reference percentiles is 0.12 Psi (Table 3), but errors are not uniformly
21 distributed. Higher percentiles tend to have larger and positive errors (a mean of 0.28 psi for
22 the Ψ_{90}), but the lowest percentiles have small negative errors (a mean of -0.011 psi for the

1 Ψ_{10}). There is a moderate amount of scatter, especially for higher percentiles, with an
2 irreducible random error of 0.21 psi. The semi-automatic sizing method produces better
3 results, with a mean error of 0.006 psi, and an irreducible random error of 0.099 psi (Fig. 10b;
4 Table 3).

5 **Figure 9.**

6 **Figure 10.**

7 **Table 3.**

8 Three key questions arise from these results. First, why does manual digitizing tend to result
9 in an overestimation of larger percentiles when sediment structure (hiding, overlapping,
10 foreshortening) might be expected to lead to the size of all grains being underestimated? This
11 effect is likely to result from three factors that work in combination to modify the grain-size
12 distributions from both the manually digitized and paint-and-pick data (the effects of which
13 are illustrated schematically in Fig. 11):

14 (a) Paint-and-pick sampling is likely to overestimate the number of small particles. This is
15 because it is difficult to unambiguously differentiate between small grains that are part
16 of the surface layer and those that are really part of the subsurface. Whilst the use of
17 spray paint to identify surface grains helps, drifting and penetration into interstices
18 may result in some subsurface grains receiving paint [*Church et al.*, 1987]. The over-
19 collection of small grains skews the paint-and-pick grain-size distribution towards the
20 fine end, leading to an underestimation of the true proportion of coarse grains and
21 reducing the size of the larger percentiles (Fig. 11a).

1 (b) Manual digitizing is likely to underestimate the number of small particles. This is
2 because they are harder to see than large grains because they are often located in
3 interstices, and they are more difficult to digitize. The effect is to skew the digitized
4 grain-size distribution towards the coarse end because of the relative overabundance of
5 easily identified larger grains (Fig 11b).

6 (c) Structural effects may also influence the digitized grain-size distributions. These
7 effects may not operate uniformly on different size fractions. Selective reduction in
8 the size of coarse grains would result in a skew to the fine end and a reduction of
9 larger percentiles (Fig. 11c). Selective reduction in the size of the small grains would
10 increase the larger percentiles (Fig 11d). Careful inspection of the images suggests
11 that small grains, many of which lie in the interstices of larger particles, are more
12 likely to exhibit foreshortening by presenting their *c*-axis to the camera than larger
13 grains, resulting in a reduction in their apparent size.

14 **Figure 11.**

15 A second question is, why does the semi-automated approach generate better results than
16 manual digitizing, which might be expected to be the ‘gold-standard’ in image-based
17 analysis? It has not been possible to provide a definitive solution to this problem. However,
18 the quality of the results from the semi-automatic method is consistent with the findings from
19 previous studies that have used fully- and partially-automatic methods [*McEwan et al.*, 2000;
20 *Butler et al.*, 2001; *Sime and Ferguson*, 2003; *Graham et al.*, 2005b]. These have identified
21 substantial under-counting of the number of particles and some attribution of individual grains
22 to the wrong size class (largely as a result of over- or under-segmentation leading to the
23 splitting or merging of grains). Nevertheless, the level of undercounting was reported to be

1 largely consistent between size classes and the levels of over- and under-estimation of the
2 sizes of individual grains approximately compensated for one another, producing size
3 distributions with small or moderate errors. The results of this study suggest that there is a
4 bias in percentiles produced by the semi-automatic measurements relative to those from
5 manual measurements, but this bias results in an improvement in the automated
6 measurements relative to the paint-and-pick control sample. Whilst this result is fortuitous, it
7 is entirely consistent with earlier work. The errors produced by the semi-automatic process
8 used here are very similar to the area-by-number errors associated with the fully automated
9 procedure of *Graham et al.* [2005b] (Table 3).

10 The third question is, why are the results from this experiment different to those from
11 previous work (which invariably report negative biases)? The answer is probably a function
12 of the way in which the data are presented and reported. Most studies have reported their
13 errors in grid-by-number form (Table 2). This requires the data to be transformed from the
14 area-by-number form in which it is collected, which may be accomplished using the
15 procedure of *Kellerhals and Bray* [1971]. Once transformed in this way, the data from this
16 study do exhibit the negative bias observed in previous studies (Fig. 12; Table 3).

17 **Figure 12.**

18 Given that the data are positively biased in area-by-number form, this negative bias in grid-
19 by-number form cannot be accounted for simply as an artefact of sediment structure. The
20 apparent change in bias is likely to result from the interaction of the nature of the grain-size
21 distributions and the transformation. *Graham et al.* [2005c] have demonstrated that the
22 conversion from area-by-number to grid-by-number data is extremely sensitive to variations
23 in the number of large grains. In an area-by-number distribution grains of all sizes have an

1 equal weighting, whereas in a grid-by-number distribution the weighing is proportional to the
2 area of the grain, so a single 128 mm grain has the same influence on the distribution as
3 around 250 8-mm grains. Adding a single large grain to the distribution can therefore
4 substantially change the shape of the cumulative distribution curve, and thus the percentiles
5 derived from it. So, the grid-by-number distributions are strongly controlled by the (relatively
6 small) number of large grains, whilst the area-by-number distributions are dominated by the
7 large numbers of smaller grains. It is possible that the size of the larger manually digitized
8 grains is underestimated as a result of structural effects, leading to the slight overall negative
9 bias. The even greater negative bias of the semi-automatic method is likely to result from
10 over-segmentation of a few of the larger grains.

11 The purpose of undertaking these experiments was to understand the importance of hiding,
12 imbrication and foreshortening on derived grain-size distributions. In practice, it has been
13 found that, whilst structural effects may be an important source of error for photographic
14 sizing methods, it is difficult or impossible to fully disentangle them from the range of other
15 factors operating, at least at the Ain River. This difficulty leads us to believe that structural
16 effects are probably small relative to the other factors operating. Although restricted to a
17 single river with a relatively limited range of structural properties, this conclusion is
18 consistent with the results of *Graham et al.* [2005b] which showed little evidence of structural
19 effects at three rivers with contrasting sediment characteristics. Nevertheless, the significance
20 of structural effects would benefit from further work, perhaps using artificially-created bed
21 structures composed of sediment with a known size distribution and a variety of camera
22 orientations to assess the importance of foreshortening.

23 **5. Interpolated versus grain-by-grain derived percentiles**

1 5.1 Rationale

2 Grain measurements associated with traditional sampling methods are most commonly made
3 with sieves or templates [e.g. *Bunte and Abt, 2001b*], although rulers, calipers, or pebble
4 boxes are sometimes used [e.g. *Ibbeken and Denzer, 1988; Marcus et al., 1995; Green, 2005*].
5 Sieves and templates have the advantage that the operator does not have to visually identify
6 the particle *b*-axis, removing a potential source of operator error. However, because these
7 methods result in each grain being classified as belonging to a particular size class, the
8 calculation of percentiles from sieve- or template-derived data requires interpolation between
9 class boundaries. This is not the case using image-based methods (or measurements by ruler,
10 caliper or pebble box) which provide information about the size of individual grains, and
11 percentiles may be determined directly from the grain-by-grain data (with interpolation only
12 required between the two grains lying on either side of the percentile of interest). Grain-size
13 percentiles obtained using interpolation between size-class boundaries are therefore not
14 exactly equivalent to those that use direct measurement of each grain.

15 Because of its computational simplicity, the most common method of calculating percentiles
16 for classified data is to use linear interpolation between class boundaries. Where the
17 cumulative curve is convex, linear interpolation results in an underestimation of the
18 percentiles; where it is concave, linear interpolation results in an overestimation of
19 percentiles. This effect is illustrated in Fig. 13a for a single sample from the River Lune,
20 England. Size data for individual grains were obtained using the automated image-processing
21 procedure of *Graham et al. [2005a, 2005b]* to produce a grain-by-grain cumulative curve. The
22 same data were placed into 1 psi classes as the basis for the interpolated curve. Different
23 results are obtained when percentiles are calculated in millimeter and psi units. In Figure 13,
24 percentiles are calculated by linear interpolation in both millimeter and psi units and then

1 plotted in psi units. Cumulative curves calculated in millimeter units have the greatest
2 deviation from the true distribution (Fig. 13b).

3 Although the interpolated cumulative grain-size curves consist of linear segments, their
4 overall ‘smoothness’ depends on the number of grain-size classes used to construct them. The
5 larger the number of classes used, the closer the derived cumulative distribution curve will be
6 to the true (grain-by-grain) curve. This means that the values of the calculated percentiles are
7 dependent on the number of size classes used. In Fig. 13, large 1 psi classes are used (rather
8 than the more usual half or quarter psi classes) to highlight the differences between the grain-
9 by-grain and interpolated curves more clearly.

10 These problems may be overcome to some extent by fitting a smooth curve through the
11 classified data. This may be achieved graphically using a draftsman’s curve, or
12 computationally using a spline-fitting algorithm. By producing a smooth cumulative curve,
13 spline interpolation results in percentiles that are closer to the true percentiles (Figure 14).
14 The results are improved for calculations made in both millimeter and psi units, although psi
15 units still produce better results. An additional advantage of spline interpolation is that it is
16 less sensitive to variations in the number of size classes used to record the data.

17 **Figure 13.**

18 **Figure 14.**

19 **5.2 Empirical assessment of the impact of interpolating percentiles**

20 To examine the likely errors associated with interpolation, a dataset consisting of 37 samples
21 for which *b*-axis measurements of every single grain are available was used. Data were

1 collected photographically, and grain measurements made using the automated procedure of
2 *Graham et al.* [2005b]. The photographic samples were collected at three rivers: River Lune,
3 England (n = 7); Afon Ystwyth, Wales (n = 15); Ettrick Water, Scotland (n = 15). Each
4 sample had an area of 1.2 m² and the number of grains larger than 3 Psi (8 mm) ranged from
5 335 to 1253 (mean = 734). Percentiles were calculated in area-by-number form (truncated at 3
6 Psi) using spline and linear interpolation with 1, 0.5, and 0.25 Psi size classes and compared
7 with percentiles calculated on a grain-by-grain basis. The results of these analyses are
8 presented in Fig. 15. As expected, errors are largest for percentiles calculated using linear
9 interpolation and with larger size classes. Substantial improvements are associated with
10 moving from 1 psi to 0.5 psi classes for both linear and spline interpolation. Improvements
11 associated with the use of 0.25 psi classes are less impressive. Similarly, the benefits of spline
12 interpolation are greatest for larger size classes. For 0.5 psi classes, spline interpolation only
13 marginally outperforms linear interpolation.

14 **Figure 15.**

15 Although the errors associated with interpolation are small where 0.5 or 0.25 psi classes are
16 used, it is generally more appropriate to use unclassified data to avoid the need for
17 interpolation when determining grain-size percentiles. This is an advantage of photographic
18 measurement techniques. Where data are obtained unavoidably in classified form,
19 interpolation should always be undertaken in psi/phi units rather than millimeters. In cases
20 where only classified data are available, it is recommended that spline interpolation be used in
21 preference to linear interpolation because it is less affected by the choice of size class.

22 **6. Summary**

1 The use of image analysis to extract surface grain-size information from images collected
2 with a hand-held digital camera is now well established [*Butler et al.*, 2001; *Sime and*
3 *Ferguson*, 2003; *Rollet et al.*, 2002; *Graham et al.*, 2005a, 2005b; *Rollet*, 2007], and can
4 provide data with a precision equivalent to conventional field-based methods. Such methods
5 have significant advantages in terms of time and cost savings, and they do not disturb the
6 substrate, making them particularly appropriate for ecological applications and monitoring
7 studies [*Graham et al.*, 2005b]. Nevertheless, there are still unresolved issues associated with
8 image collection, extraction of grain-size information, and analysis of the resulting data (Fig.
9 1). This paper represents the first attempt to address several issues related to the deployment
10 of image-based methods (although many of the results are also of relevance to traditional
11 grain-sizing methods). It is anticipated that this information will assist practitioners in making
12 appropriate operational decisions to maximize the quality of the information obtained by
13 image-based methods.

14 It has been found that sampling areas of less between 200- and 400-times the area of the
15 largest grain are required for characterizing the full grain-size distribution of the Afon
16 Ystwyth, producing errors in percentiles of less than 5% (in mm). Where information on the
17 coarse part of the distribution is not required, areas of between 100- and 200-times that of the
18 largest grain are adequate for characterizing the median grain size. The areas can be halved if
19 errors of less than 10% (in mm) are acceptable. These results do not support the theoretical
20 work of *Petrie and Diplas* [2000], who argued that sample areas smaller than 100-times that
21 of the largest grain are acceptable. Although the results are for a single site with a relatively
22 restricted range of sediment characteristics, it seems likely that larger sample areas (as
23 recommended by *Diplas and Fripp* [1992] and *Fripp and Diplas* [1993]) are appropriate.

1 The investigations of the impact of truncation at the fine end of the distribution indicate that
2 this has a relatively small impact on higher percentiles where the sample contains less than
3 5% sand. For these samples, the mean error in the D_{50} associated with truncation at 8 mm was
4 -4.2% (in mm) (based on 66 samples). For samples with larger quantities of fines, errors were
5 larger, but may still be acceptable depending on the application. These results indicate that
6 truncation should be applied with care, with due regard to the purpose of the study. Where the
7 fine part of the grain-size distribution is of particular interest (e.g. in assessment of habitat
8 suitability for salmon spawning), truncation may be inappropriate. However, comparisons
9 between data sets must always be made on a like-with-like basis, and truncation may be
10 essential to facilitate the comparison of datasets collected by different methods. For image-
11 based sampling methods, these results highlight the need to collect images at an appropriate
12 resolution bearing in mind the minimum resolvable grain size required for the application
13 [Church *et al.*, 1987]. The relation between camera resolution, minimum resolvable grain size
14 and area photographed are discussed by Graham *et al.* [2005a, 2005b].

15 Attempts to assess the impact of sediment structure on grain-size distributions obtained by
16 photographic sampling have been complicated by a range of other factors in operation. The
17 analysis has highlighted the fact that no technique provides a definitive assessment of the
18 surface grain-size distribution. All techniques are subject to biases of one kind or another, and
19 these make assessments of procedure performance challenging because there is no universally
20 appropriate benchmark against which errors may be evaluated. In this regard, fully-automated
21 image-based methods have a significant advantage over alternatives because they do not
22 require any user intervention and are thus free of operator-introduced bias. Such biases are
23 likely to be greatest where inexperienced operators are used, whereas image-based data
24 collection may be undertaken successfully with limited training. The analysis suggests that

1 the magnitude of errors, associated with structural effects, are small relative to other factors,
2 but further work is desirable to explore this issue further.

3 Although the errors introduced by interpolating percentiles between the boundaries of size
4 classes are likely to be small, measurements of individual grains enable percentiles to be
5 calculated directly and more accurately (provided that the measurements of the individual
6 grains are accurate). A particular disadvantage of interpolated percentiles is that the results are
7 partially dependent on how big the size classes are. Because they measure grains individually,
8 image-based methods therefore offer advantages over techniques that allocate grains to size
9 classes, without the time overhead associated with measurements using a ruler, calipers or
10 pebble box. Where size data are unavoidably obtained in classified form, errors are minimized
11 by calculating percentiles in psi/phi units (rather than millimeters) and by using spline rather
12 than linear interpolation.

13 **Acknowledgements**

14 Thanks to Gordon Grant and four anonymous referees whose comments have resulted in
15 improvements to the manuscript. Thanks also to the numerous assistants over many years who
16 have helped us collect the data presented. The work was facilitated by a travel grant to DJG
17 by Loughborough University.

18 **References**

19 Adams, J. (1979), Gravel size analysis from Photographs, *J. Hydraul. Div. Am. Soc. Civ.*
20 *Eng.*, 105, 1247-1255.

- 1 Adams, P. N., P. Ruggiero, G. C. Schoch, and G. Gelfenbaum (2007), Intertidal sand body
2 migration along a megatidal coast, Kachemak Bay, Alaska, *J. Geophys. Res.*, *112*, F02007,
3 doi:10.1029/2006JF000487.
- 4 Bunte, K., and S. R. Abt (2001a), Sampling surface and subsurface particle-size distributions
5 in wadable gravel-and cobble-bed streams for analyses in sediment transport, hydraulics,
6 and streambed monitoring, *Gen. Tech. Rep. RMRS-GTR-74*, 428 pp., U.S. Department of
7 Agriculture, Forest Service, Rocky Mountain Research Station, Fort Collins, CO.
- 8 Bunte, K., and S. R. Abt (2001b), Sampling frame for improving pebble count accuracy in
9 coarse gravel-bed streams, *J. Am. Water Resour. Assoc.*, *37*, 1001-1014.
- 10 Buscombe, D., and G. Masselink (2009), Grain size information from the statistical properties
11 of digital images of sediment, *Sedimentology*, *56*, 421-438.
- 12 Butler, J. B., S. N. Lane, and J. H. Chandler (2001), Automatic extraction of grain-size data
13 from gravel surfaces using digital image processing, *J. Hydraul. Res.*, *39*, 519-529.
- 14 Carbonneau, P. E. (2005), The threshold effect of image resolution on image-based automated
15 grain size mapping in fluvial environments. *Earth Surf. Processes Landforms*, *30*, 1687-
16 1693.
- 17 Carbonneau, P. E., S. N. Lane, and N.E. Bergeron (2004), Catchment-scale mapping of
18 surface grain size in gravel bed rivers using airborne digital imagery, *Water Resour. Res.*,
19 *40*(7), W07202, doi:10.1029/2003WR002759.

- 1 Chandler, J. H., S. P. Rice, and M. Church (2004), Colour aerial photography for riverbed
2 classification, *Archives of the International Society for Photogrammetry and Remote*
3 *Sensing*, Volume XXXV, Part VII.
- 4 Church, M. A., D. G. McLean, and J. F. Wolcott (1987), River bed gravels: Sampling and
5 analysis, in *Sediment Transport in Gravel-bed Rivers*, edited by C. R. Thorne et al., pp. 43-
6 79, John Wiley, Hoboken, N. J.
- 7 De Vries, M. (1970), On the accuracy of bed-material sampling, *J. Hydraul. Res.*, 8, 523-533.
- 8 Digabel H. and C. Lantuejoul (1977), Iterative algorithms, *ENSMP Eds, Centre de*
9 *géostatistique et de morphologie mathématique*, 16 p.
- 10 Diplas, P., and J. B. Fripp (1992), Properties of various sediment sampling procedures, *J.*
11 *Hydraul. Eng.*, 118, 955-970.
- 12 Fripp, J. B., and P. Diplas (1993), Surface sampling in gravel streams, *J. Hydraul. Eng.*, 119,
13 473-490.
- 14 Graham, D. J., I. Reid, and S. P. Rice, (2005a), Automated sizing of coarse-grained
15 sediments: Image-processing procedures, *Mathematical Geology*, 37, 1-28.
- 16 Graham, D. J., S. P. Rice, and I. Reid (2005b), A transferable method for the automated grain
17 sizing of river gravels. *Water Resour. Res.*, 41, W07020, doi: 10.1029/2004WR003868.

- 1 Graham, D. J., S. P. Rice, and I. Reid (2005c), Comment: Photographic techniques for
2 characterizing streambed particle sizes, *Transactions of the American Fisheries Society*,
3 *134*, 1599-1603.
- 4 Green, J.C. (2005), Choice of percentiles and axes to determine grain resistance, *J. Hydraul.*
5 *Eng.*, *131*, 1007-1010.
- 6 Haschenburger, J. K., S. P. Rice, and E. Voight (2007), Evaluation of bulk sediment sampling
7 criteria for gravel-bed rivers, *J. Sedimentary Res.*, *77*, 415-423, doi: 10.2110/jsr.2007.040.
- 8 Hedger, R. D., J. J. Dodson, J. F. Bourque, N. E. Bergeron, and P. E. Carbonneau (2006),
9 Improving models of juvenile Atlantic salmon habitat use through high resolution remote
10 sensing, *Ecological Modelling*, *197*(4): 505–511.
- 11 Ibbeken, H., and P. Denzer (1988) Clast measurement: a simple manual device and its
12 semiautomatic electronic equivalent, *J. Sedimentary Petrology*, *58*, 751-752.
- 13 Ibbeken, H., and R. Schleyer (1986), Photo-sieving: A method for grain-size analysis of
14 coarse-grained, unconsolidated bedding surfaces, *Earth Surf. Processes Landforms*, *23*,
15 481-492.
- 16 Inman, D. L. (1952), Measures for describing the size distribution of sediments. *J.*
17 *Sedimentary Petrology*, *22*, 125-145.
- 18 Kellerhals, R., and D. I. Bray (1971), Sampling procedures for coarse fluvial sediments. *J.*
19 *Hydraul. Div. Am. Soc. Civ. Eng.*, *97*, 1165-1180.

- 1 Kondolf, G. M., T. E. Lisle, and G. M. Wolman (2003), Bed sediment measurement, in Tools
2 in Fluvial Geomorphology, edited by G. M. Kondolf and H. Piégay, pp. 347-395, John
3 Wiley, Chichester.
- 4 Lane, E. W., and E. J. Carlson (1953), Some factors affecting the stability of canals
5 constructed in coarse granular material, in *Proceedings of the 5th IAHR Congress*, pp 37-
6 48, Int. Assoc. of Hydraul. Res., Madrid.
- 7 Marcus, W. A., and M. A. Fonstad (2008), Optical remote mapping of rivers at sub-metre
8 resolutions and watershed extents. *Earth Surf. Processes Landforms*, 33, 4-24.
- 9 Marcus, W. A., S. C. Ladd, J. A. Stoughton, and J. W. Stock (1995), Pebble counts and the
10 role of user-dependent bias in documenting sediment size distributions. *Water Resour.*
11 *Res.*, 31, 2625-2631.
- 12 McEwan, I. K., T. M. Sheen, G. T. Cunningham, and A. R. Allen (2000), Estimating the size
13 composition of sediment surfaces through image analysis, *Proc. Inst. Civ. Eng. Water Mar.*
14 *Energy*, 142, 189-195.
- 15 Petrie, J., and P. Diplas (2000), Statistical approach to sediment sampling accuracy, *Water*
16 *Resour. Res.*, 36, 597-605.
- 17 Reid, I., S. Rice, and C Garcia (2001), Discussion of “The measurement of gravel-bed river
18 morphology”, in *Gravel-Bed Rivers V*, edited by M. P. Mosley, pp. 325-327, N. Z. Hydrol.
19 Soc., Wellington.

- 1 Reid, I., D. M. Powell, and J. B. Laronne (1996), Prediction of bedload transport by desert
2 flash-floods, *Journal of Hydraulic Engineering, American Society of Civil Engineers*, 122,
3 170-173.
- 4 Rice, S. P. (1995), The spatial variation and routine sampling of spawning gravels in small
5 coastal streams, *Working Paper 06/1995*, 41 pp., Research Branch, British Columbia
6 Ministry of Forests, Victoria, BC.
- 7 Rice, S., and M. Church (1996), Sampling surficial fluvial gravels: The precision of size
8 distribution percentile estimates, *J. Sediment. Res.*, 66, 654-665.
- 9 Rice, S. P., and J. K. Haschenburger (2004), A hybrid method for size-characterisation of
10 coarse subsurface fluvial sediments, *Earth Surf. Processes Landforms*, 29, 373-389.
- 11 Rollet, A. J. (2007), Etude et gestion de la dynamique sédimentaire d'un tronçon fluvial à
12 l'aval d'un barrage: le cas de la basse vallée de l'Ain, Thèse de doctorat de géographie,
13 305 pp., Université de Lyon, Lyon.
- 14 Rollet, A. J., B. Kauffmann, H. Piégay, and B. Lacaze (2002), Automated calculation of grain
15 size percentiles using image analysis: example of the bars of the Ain River (France), paper
16 presented at the River Bed Patches: Hydraulics, Ecology and Geomorphology, The British
17 Hydrological Society, Loughborough, UK, 8 May 2002.
- 18 Rubin, D. M. (2004), A simple autocorrelation algorithm for determining grain size from
19 digital images of sediment, *J. Sediment. Res.*, 74, 160-165.

- 1 Ruggiero, P., P. N. Adams, and J. A. Warrick (2007), Mixed sediment beach
2 processes: Kachemak Bay, Alaska, in *Coastal Sediments '07: Proceedings of 6th*
3 *International Symposium on Coastal Engineering and Science of Coastal Sediment*
4 *Processes*, p. 14, American Society of Civil Engineers, New Orleans, LA.
- 5 Sime, L. C. and R. I. Ferguson (2003), Information on grains sizes in gravel-bed rivers by
6 automated image analysis, *J. Sediment. Res.*, 73, 630-636.
- 7 Soille, P. (2002), *Morphological Image Analysis: Principles and Applications*, 2nd ed., 391
8 pp., Springer-Verlag, Berlin.
- 9 Verdu, J. M., R. J. Batalla, and J. A. Martínez-Casasnovas (2005), High-resolution grain-size
10 characterization of gravel bars using image analysis and geo-statistics. *Geomorphology*,
11 72, 73-93.
- 12 Wolman, M. G. (1954), A method of sampling coarse river-bed material, *Trans. AGU*, 35,
13 951-956.
- 14

1 **Figure captions**

2 **Figure 1.** The three steps in deriving grain-size information from ground-based digital
3 photographs, illustrating some key procedural questions associated with each. Questions
4 highlighted in bold are addressed in this paper.

5 **Figure 2.** Covariant plot of percentile errors (area-by-number) versus the ratio between
6 sampled area and the area of the largest grain in the population (D_{\max}). The shaded region
7 indicates an error of less than 5% in mm (equivalent to an error of less than 0.07 Psi). (a)
8 Errors in the median grain size (D_{50}). (b) Errors in the D_{90} grain size.

9 **Figure 3.** Covariant plot of percentile errors versus the ratio between sampled area and the
10 area of the largest grain (D_{\max}). The shaded region indicates an error of less than 5% in mm
11 (equivalent to an error of less than 0.07 Psi). (a) Errors in the median grain size (D_{50}). (b)
12 Errors in the D_{90} grain size.

13 **Figure 4.** The grain-size distribution of 74 grid-by-number samples. Solid lines represent
14 samples with <5% sand ($n = 66$), and dashed lines represent samples with >5% sand ($n = 8$).
15 Data are for Fraser ($n = 19$), Chilliwack ($n = 11$) and Peace ($n = 44$) Rivers. Mean sample size
16 = 304 grains (standard deviation = 25 grains). All samples recorded at 0.5 Psi intervals down
17 to 1 Psi (2 mm), and the presence of smaller grains tallied.

18 **Figure 5.** The effect of truncation at (a) 1 Psi (2 mm), (b) 3 Psi (8 mm), and (c) 5 Psi (16 mm)
19 for the 74 grid-by-number samples. Upper panels show the difference between true and
20 truncated percentiles for each sample. Lower panels show the mean error in every 5th
21 percentile, with error bars representing the standard error. In both panels, the solid line

1 represents samples with <5% sand (n = 66), the dashed line represents samples with >5%
2 sand (n = 8). The shaded area indicates an error of less than 0.5 Psi.

3 **Figure 6.** Illustration of the three potential sources of grain size underestimation resulting
4 from sediment structure and the use of photographic sampling methods. (a) Partial burying of
5 grains. (b) Overlapping of grains as a result of imbrication. (c) Foreshortening of grains as a
6 result of projection onto a horizontal plane.

7 **Figure 7.** Example 0.6 m² sediment patch and manually digitized grain boundaries.

8 **Figure 8.** The number of grains identified in 0.5 psi size classes using image-based methods
9 compared to paint-and-pick sampling. (a) Manual digitizing with Adobe® Illustrator®. (b)
10 Semi-automated grain identification using the procedure of *Rollet et al.* [2002].

11 **Figure 9.** Area-by-number grain-size distribution for one of the sample patches derived by
12 paint-and-pick sampling and manual digitization. (a) Histogram illustrating the number of
13 grains in 0.5 Psi sieve classes. Note that manual digitizing finds a larger proportion of the
14 large grains relative to the smaller grains. (b) The resulting cumulative grain-size distribution
15 curves.

16 **Figure 10.** Area-by-number percentiles defined by image analysis and paint-and-pick
17 sampling. (a) Manual digitization vs paint-and-pick sampling. (b) Semi-automated analysis vs
18 paint-and-pick sampling.

19 **Figure 11.** Schematic representation of the effect on cumulative grain-size curves of biases
20 operating on paint-and-pick and manually digitized data. (a) Overestimation of the number of
21 small grains by paint-and-pick sampling. (b) Underestimation of the number of small grains

1 by manual digitization. (c) Underestimation of the size of large grains by manual digitization,
2 as a result of sediment structure. (d) Underestimation of the size of small grains by manual
3 digitization as a result of sediment structure.

4 **Figure 12.** Grid-by-number percentiles defined by image analysis and paint-and-pick
5 sampling. (a) Manual digitization vs paint-and-pick sampling. (b) Semi-automated analysis vs
6 paint-and-pick sampling.

7 **Figure 13.** Example of the errors associated with using linear interpolation on classified data
8 to calculate grain-size percentiles. Solid lines indicated the true grain-by-grain distribution
9 derived using the photographic method of *Graham et al.* [2005b] and with a lower truncation
10 of 3 Psi (8 mm). Dotted lines indicate the distribution based on placing the same data in 1 Psi
11 classes and interpolating percentiles in mm units. Dashed lines indicate the distribution based
12 on 1 Psi classes and interpolation percentiles in Psi units. (a) Cumulative grain-size
13 distributions. (b) Deviations from the true grain-size distribution associated with linear
14 interpolation.

15 **Figure 14.** Example of the errors associated with using spline interpolation on classified data
16 to calculate grain-size percentiles. Solid lines indicated the true grain-by-grain distribution
17 derived using the photographic method of *Graham et al.* [2005b] and with a lower truncation
18 of 3 Psi (8 mm). Dotted lines indicate the distribution based on placing the same data in 1 Psi
19 classes and interpolating percentiles in mm units. Dashed lines indicate the distribution based
20 on 1 Psi classes and interpolation percentiles in Psi units. (a) Cumulative grain-size
21 distributions. (b) Deviations from the true grain-size distribution associated with spline
22 interpolation.

1 **Figure 15.** The errors associated with the use of linear and spline interpolation in psi units on
2 classified data to calculate grain-size percentiles for 37 samples. The errors presented are
3 absolute errors; actual errors may be positive or negative. Data are derived from photographs
4 using the method of *Graham et al.* [2005b] with a lower truncation of 3 Psi (8 mm) and are
5 presented in area-by-number form. Note that the vertical scale is the same in all plots.

1 **Tables**

2 **Table 1.** Sampling areas required for areal sampling relative to the population D_{\max} grain
3 size.

Precision	Area-by-number data		Grid-by-number data	
	D₅₀	D₉₀	D₅₀	D₉₀
5% in mm (0.07 Psi)	100 times	200 times	200 times	400 times
10% in mm (0.14 in Psi)	50 times	100 times	100 times	200 times

1 **Table 2.** Reported bias in image-based grain-size measurements.

Source	Method of grain measurement	Absolute bias (Psi)¹	Percentage bias (mm)¹	Basis of comparison
<i>Kellerhals and Bray</i> [1971]	Unreported	0.26 Psi	20%	Grid-by-number
<i>Adams</i> [1979]	Manual measurement with a ruler on enlarged photograph	0.1 Psi	7 %	Grid-by-number/ area-by-number ²
<i>Ibbeken and Schleyer</i> [1986]	Photo-sieving: manual digitizing followed by estimation of grain weight	0.24 Psi	18%	Area-by-weight
<i>Bray</i> [1972], cited in <i>Church et al.</i> [1987]	Unreported	0.29 Psi (for D50)	22% (for D50)	Grid-by-number
<i>Butler et al.</i> [2001]	Semi-automated digital analysis	0.13 – 0.33 Psi	9.4 – 26.7%	Selected grains
<i>Sime and Ferguson</i> [2003]	Semi-automated digital analysis	1.11 – 1.34 Psi ³	115 – 153% ³	Grid-by-number
<i>Graham et al.</i> [2005b]	Fully automated digital analysis	0.007 – 0.03 Psi 0.10 – 0.17 Psi	0.5 – 2.1% 7.2 – 12.5%	Area-by-number Grid-by-number

2

1 Notes:

2 ¹Bias is invariably negative (i.e. photographic methods underestimate the true size).

3 ²*Adams* [1979] made an invalid comparison between photographic grid-by-number data and
4 area-by-weight data derived from paint-and-pick sampling [*Kondolf et al.*, 2003].

5 ³*Graham et al.* [2005b] found a coding error in the algorithm used by *Sime and Ferguson*
6 [2003] for converting from area-by-number to grid-by-number. It is likely that stated biases
7 are significantly overestimated, and likely to be closer to those of *Graham et al.* [2005b].

8

1 **Table 3.** Errors associated with manual digitizing and semi-automated image analysis.

	Area-by-number		Grid-by-number	
	Manual digitizing errors (psi)	Semi-automated errors (psi)	Manual digitizing errors (psi)	Semi-automated errors (psi)
D ₁₀ mean error	-0.011	-0.028	0.184	-0.092
D ₁₆ mean error	-0.004	-0.030	0.191	-0.138
D ₂₅ mean error	0.018	-0.029	0.158	-0.232
D ₅₀ mean error	0.091	0.049	-0.013	-0.489
D ₇₅ mean error	0.217	0.078	-0.158	-0.595
D ₈₄ mean error	0.252	0.048	-0.361	-0.664
D ₉₀ mean error	0.279	-0.047	-0.434	-0.668
Mean error or Bias, b	0.120	0.006	-0.062	-0.411
Mean-square error, E_{ms}	0.058	0.010	0.189	0.272
Irreducible random error, e	0.209	0.099	0.430	0.322

2

3 Note: Grid-by-number data are obtained by converting the area-by-number data using the
 4 procedure of *Kellerhals and Bray* [1971].

5

Step 1

Collection of photos
<p>What sampling area is required?</p> <p>What internal camera settings (focal length, resolution etc.) are required? [Graham et al., 2005a]</p> <p>What external camera configuration (elevation, flash etc.) is required? [Graham et al., 2005b]</p> <p>What type of illumination is required? [Graham et al., 2005b]</p> <p>What image resolution is required? [Graham et al., 2005a]</p>

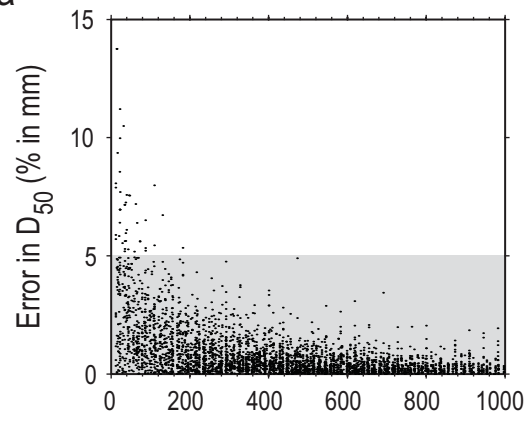
Step 2

Extraction of grains
<p>What is the size of the minimum grain identifiable? [Graham et al., 2005a]</p> <p>Consequently: What effect does truncation have on the resulting size distribution?</p> <p>Does bed structure affect the grain-size distribution?</p> <p>How should particles touching the edges of the photo be treated? [Graham et al., 2005b]</p> <p>What errors are associated with the grain extraction & measurement algorithms? [Graham et al., 2005a,b]</p>

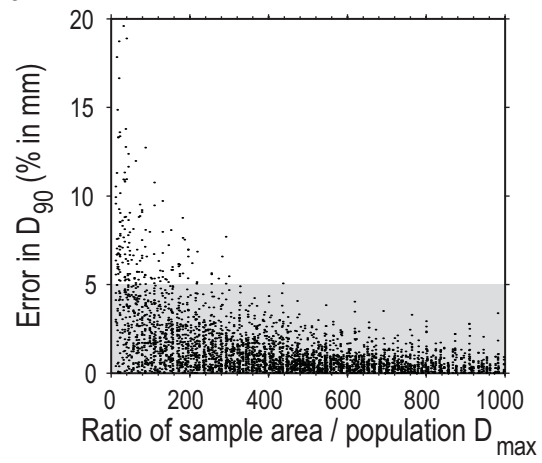
Step 3

Analysis of results
<p>Does the method of calculating percentiles affect the results?</p>

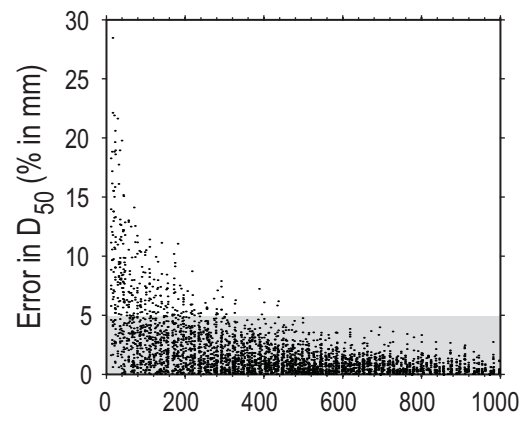
a



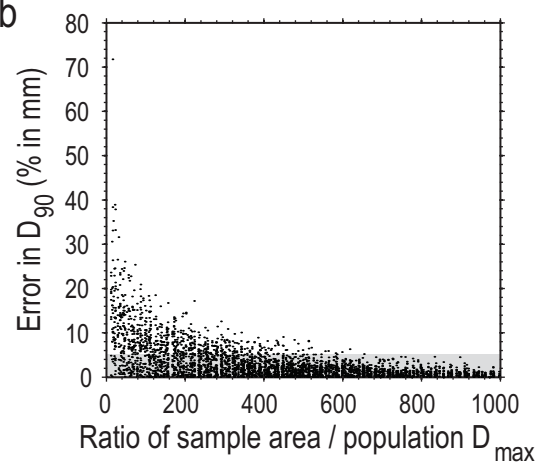
b

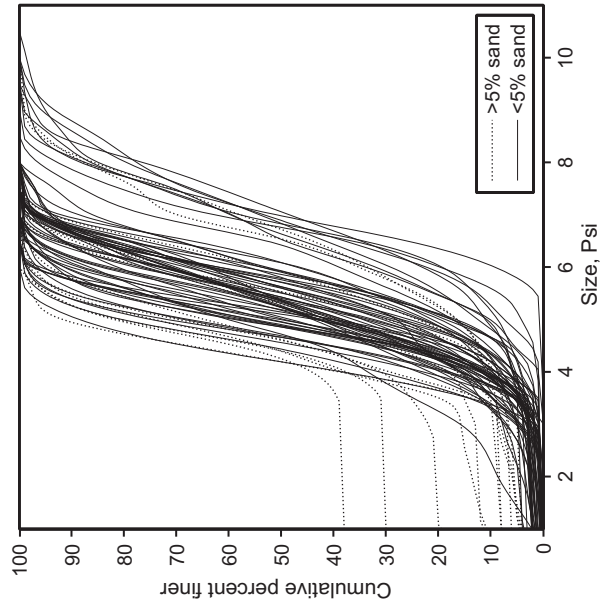


a

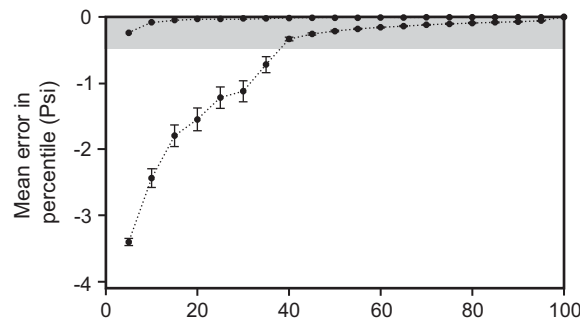
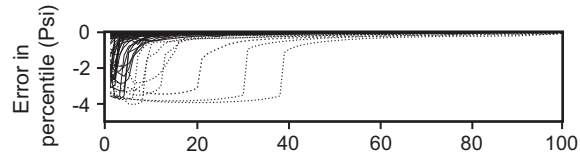


b

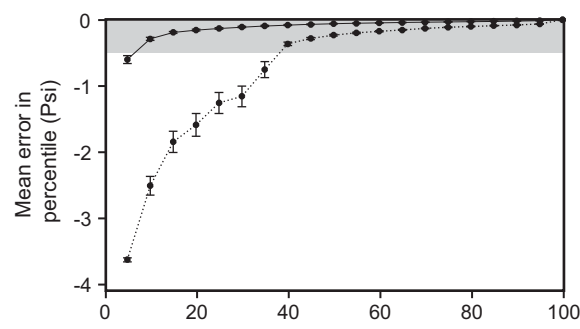
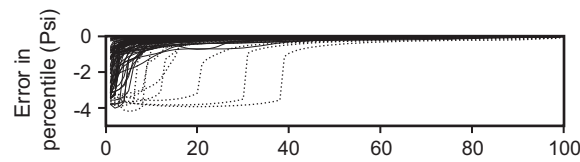




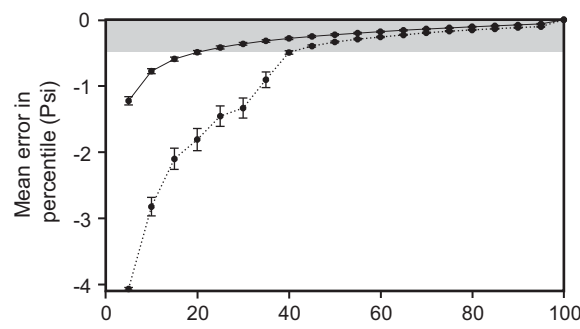
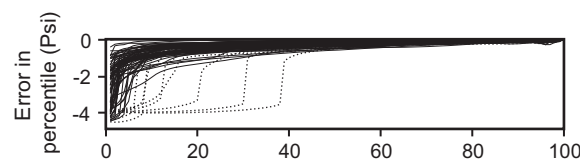
a



b

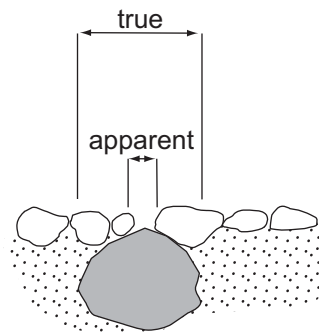


c

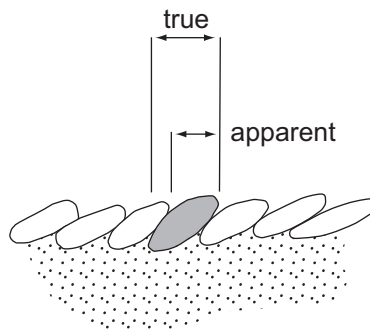


Percentile

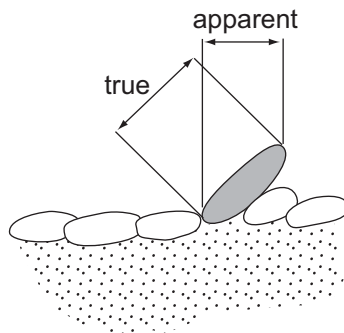
a) Burial

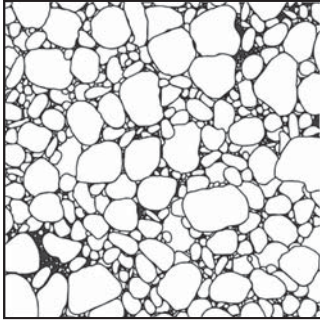
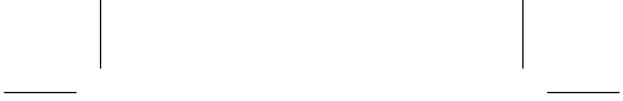


b) Overlapping



c) Foreshortening





b



a



